Electronic Supplementary Material (ESI) for Energy & Environmental Science.

Supplementary Information

Effect of Alkyl Substitution Position of Thienyl Outer Side Chains on Photovoltaic Performance of the A-DA'D-A Type Acceptors

Xiaolei Kong[a,b], Can Zhu[a,b], Jinyuan Zhang[a], Lei Meng[a,b], Shucheng Qin[a,b], Jianqi Zhang[c], Jing Li[d], Zhixiang Wei[c], Yongfang Li[a,b,e*]*

[a] Beijing National Laboratory for Molecular Sciences, CAS Key Laboratory of Organic Solids, Institute of Chemistry, Chinese Academy of Sciences, Beijing 100190, China

[b] School of Chemical Science, University of Chinese Academy of Sciences, Beijing 100049, China

[c] CAS key laboratory of nanosystem and hierarchical fabrication, CAS Center for Excellence in Nanoscience, National Center for Nanoscience and Technology, 100190 Beijing, China

[d] Key Laboratory of Photochemical Conversion and Optoelectronic Materials, Technical Institute of Physics and Chemistry, Chinese Academy of Sciences, Beijing 100190, China

[e] Laboratory of Advanced Optoelectronic Materials, Suzhou Key Laboratory of Novel Semiconductor Materials and Devices, College of Chemistry, Chemical Engineering and Materials Science, Soochow University, Suzhou, Jiangsu 215123, China

[*]**Corresponding authors:** menglei@iccas.ac.cn (L. Meng), liyf@iccas.ac.cn (Y. Li)

Experimental Section

1.Synthetic Procedures of *m*-TEH and *o*-TEH

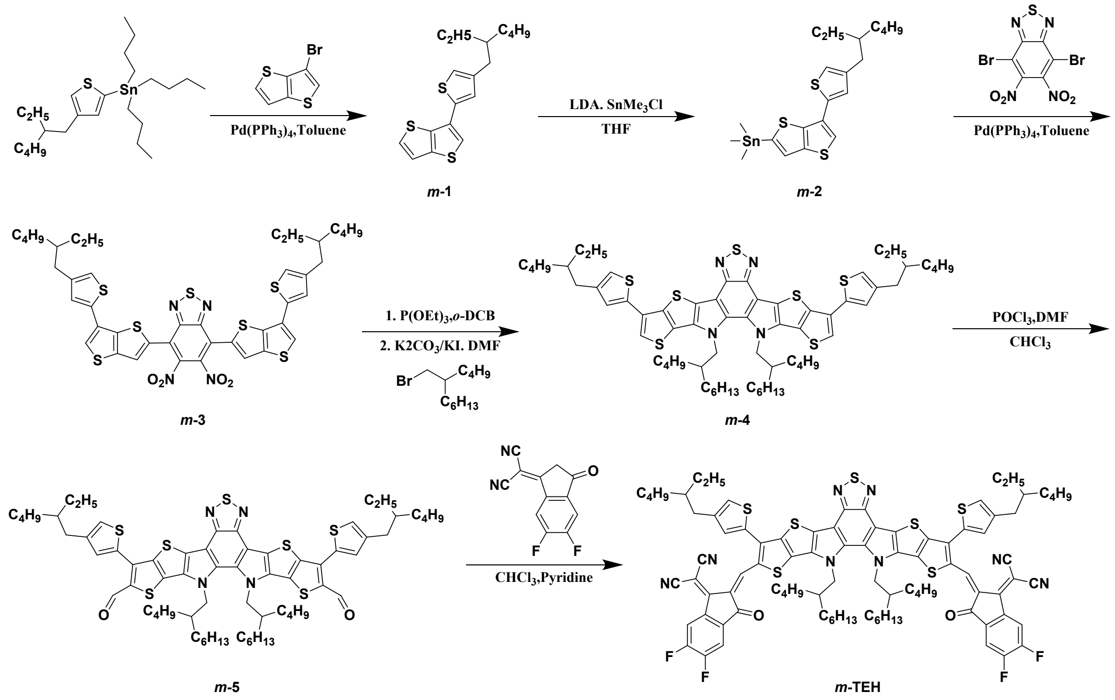

Scheme S1. Synthetic route of *m*-TEH

Synthetic route of *m*-TEH is shown in **Scheme S1**. The detailed synthesis processes are described in the following.

Synthesis of compound *m*-1

A mixture of compound tributyl(4-(2-ethylhexyl)thiophen-2-yl)stannane (4.00 g, 8.24 mmol), 3-bromothieno[3,2-b]thiophene (1.85 g, 8.45 mmol), and $Pd(PPh_3)_4$ (0.35 g, 0.30 mmol) were dissolved in anhydrous toluene (40.0 mL) and stirred at 110 °C overnight under argon atmosphere. After being cooled to room temperature, the solvent was then removed under reduced pressure. The residue was washed with water and extracted with hexane. Without any further purification, the product was used into the following reaction.

Synthesis of compound *m*-2

To a solution of compound ***m*-1** in anhydrous tetrahydrofuran (40 mL), 2.0 **M** lithium diisopropylamide (3.0 mL, 6.0 mmol) was added dropwise at -78 °C under argon atmosphere. After stirring at the same temperature for 3.5 h, 1.0 **M** trimethyltin chloride (6.0 mL, 6.0 mmol) was added dropwise at -78 °C, and the mixture was gradually warmed to room temperature. After stirring overnight, the mixture was quenched with saturated KF aqueous solution and extracted with hexane. The organic layer was dried with Na_2SO_4. Removing the solvent under reduced pressure gave the crude compound ***m*-2**. Without any further purification, the product was used into the following reaction.

Synthesis of compound *m*-3

Compound ***m*-2**, 4,7-dibromo-5,6-dinitrobenzo[c][1,2,5]thiadiazole (0.96 g, 2.5 mmol), and $Pd(PPh_3)_4$ (0.20 g, 0.17 mmol) were dissolved in anhydrous toluene(25.0 mL) and stirred at 110 °C overnight under argon atmosphere. Then, the reaction mixture was cooled and poured into a saturated KF aqueous solution. The mixture was extracted with diethyl ether for three times. The combined organic phase was washed with water followed by brine. Then, the solution was dried over Na_2SO_4 and concentrated under reduced pressure. Compound ***m*-3** was purified by chromatography in on a silica gel column eluting with petroleum ether/dichloromethane (3/1, *v*/*v*), which yields a red powder as product (1.74 g, 78% yield). ^1H NMR (300 MHz, $CDCl_3$) δ 7.72 (s, 2H), 7.59 (s, 2H), 7.21 (s, 2H), 6.89 (s, 2H), 2.60 (d, J = 6.9 Hz, 4H), 1.72 – 1.54 (m, 13H), 1.44 – 1.24 (m, 42H), 0.92 (q, J = 6.8 Hz, 33H). ^{13}C NMR (75 MHz, $CDCl_3$) δ 152.19, 143.04, 141.97, 141.69, 139.59, 136.07, 131.14, 128.76, 126.26, 124.45, 123.84, 121.46, 120.52, 40.43, 34.66, 32.63, 29.04, 28.40, 26.89, 25.77, 23.18, 17.42, 14.30, 14.27, 13.71, 11.00.

Synthesis of compound *m*-4

Compound ***m*-3** (1.74 g, 1.95 mmol) and triethyl phosphate (10 mL) were dissolved in anhydrous 1,2-dichlorobenzene (*o*-DCB, 10 mL) under argon and the mixture was stirred at 180 °C overnight. After cooling to room temperature, the solvent was removed by vacuum distillation. Subsequently, the red intermediate was then mixed with K_2CO_3 (2.70 g, 19.5 mmol), KI (0.32 g, 1.95 mmol), 5-(bromomethyl)decane (1.46 g, 5.85 mmol), and anhydrous DMF (25 mL) were mixed under argon and stirred at 100 °C overnight. The mixture was extracted with ethyl acetate ether for three times. The combined organic phase was washed with water followed by brine. Then, the solution was dried over Na_2SO_4 and concentrated under reduced pressure to yield an orange oil. Compound ***m*-4** was obtained by column chromatography on silica gel using petroleum ether/dichloromethane (6/1, *v*/*v*) as the eluent to give an orange solid (1.04 g, 46% yield). ^1H NMR (300 MHz, $CDCl_3$) δ 7.47 (s, 2H), 7.39 (s, 2H), 6.91 (s, 2H), 4.63 (d, J = 7.8 Hz, 4H), 4.03 (d, J = 5.9 Hz, 10H), 2.63 (d, J = 7.0 Hz, 4H), 2.09 (p, J = 6.4 Hz, 2H), 1.66 (q, J = 6.1 Hz, 7H), 1.47 – 1.18 (m, 97H), 1.16 – 0.54 (m, 91H). ^{13}C NMR (75 MHz, $CDCl_3$) δ 155.78, 147.62, 143.07, 139.39, 136.69, 136.27, 131.98, 130.25, 126.28, 124.42, 120.19, 118.73, 111.61, 70.80, 55.15, 40.32, 38.78, 37.45, 34.83, 32.54, 31.82, 31.54, 31.01, 30.68, 30.43, 30.31, 30.16, 29.61, 29.34, 29.31, 28.92, 28.88, 28.04, 27.86, 26.64, 25.67, 25.33, 25.14, 23.15, 22.98, 22.76, 22.72, 22.66, 22.46, 22.44, 14.20, 14.09, 14.05, 13.93, 13.91, 13.76, 13.73, 10.85.

Synthesis of compound *m*-5

Compound ***m*-4** (1.04 g, 0.90 mmol) was dissolved in 20 mL trichloromethane under argon, then the fresh Vilsmeier reagent (3.3 mL $POCl_3$ in 6.9 mL DMF) was added dropwise at 0 °C. After stirring for 20 min at 0 °C, the mixture was heated to 65 °C and reacted 24 h. The reaction was quenched with saturated $NaHCO_3$ solution and allowed to stir at room temperature for 24 h. The organic layer was separated, and the aqueous phase was extracted with diethyl ether for three times. The combined organic layer was washed with brine, dried over Na_2SO_4, filtered, and concentrated under reduced pressure. The crude product was purified with column chromatograph on silica gel using petroleum ether/dichloromethane (1/1, *v*/*v*) as the eluent to give an orange solid ***m*-5** (889.0 mg, 81% yield). ^1H NMR (300 MHz, $CDCl_3$) δ 10.26 (s, 2H), 7.42 (s, 2H), 7.20 (s, 2H), 4.79 – 4.55 (m, 4H), 2.68 (d, J = 6.8 Hz, 4H), 2.06 (p, J = 6.3 Hz, 2H), 1.66 (p, J = 6.7, 6.2 Hz, 2H), 1.47 – 1.21 (m, 17H), 1.21 – 0.48 (m, 60H). ^{13}C NMR (75 MHz, $CDCl_3$) δ 183.72, 147.49, 143.55, 142.62, 137.93, 137.00, 136.81, 133.04, 132.26, 131.56, 129.28, 128.17, 124.42, 112.55, 55.39, 53.43, 40.46, 39.01, 34.57, 32.59, 31.52, 30.41, 30.24, 30.04, 29.33, 28.97, 28.01, 27.82, 25.72, 25.25, 25.03, 23.10, 22.77, 22.72, 22.46, 14.19, 13.94, 13.75, 13.72, 10.90.

Synthesis of compound *m*-TEH

Compound ***m*-5** (50.0 mg, 0.04 mmol), 2-(5, 6-difluoro-3-oxo-2, 3-dihydro-1H-inden-1-ylidene) malononitrile (110.7 mg, 0.48 mmol), pyridine (1.0 mL), and chloroform (10.0 mL) were dissolved in a round bottom flask under nitrogen. The mixture was stirred at room temperature overnight, then the mixture was poured intomethanol and filtered. The residue was purified with column chromatography on silica gel using dichloromethane/petroleum ether (1/1, v/v) as the eluent to give a dark blue solid ***m*-TEH** (48.7 mg, 74% yield). ^{1}H NMR (300 MHz, CDCl$_3$) δ 9.13 (d, J = 3.9 Hz, 2H), 8.54 (dt, J = 10.7, 5.0 Hz, 2H), 7.71 (tt, J = 7.2, 3.5 Hz, 2H), 7.35 (d, J = 4.4 Hz, 4H), 4.90 – 4.64 (m, 4H), 2.72 (d, J = 6.1 Hz, 4H), 2.14 (s, 2H), 1.68 (s, 2H), 1.48 – 0.47 (m, 72H). ^{13}C NMR (75 MHz, CDCl$_3$) δ 158.93, 147.47, 144.45, 144.39, 144.18, 138.43, 137.53, 134.80, 134.12, 133.72, 133.14, 132.32, 131.73, 126.41, 121.43, 114.96, 114.58, 113.80, 113.57, 112.63, 69.53, 55.74, 40.40, 39.32, 34.53, 32.56, 31.60, 30.62, 30.50, 30.36, 29.46, 29.41, 29.00, 28.18, 27.97, 25.62, 25.44, 25.21, 23.12, 22.88, 22.82, 22.50, 22.48, 14.23, 14.01, 13.99, 13.82, 13.78, 10.91.

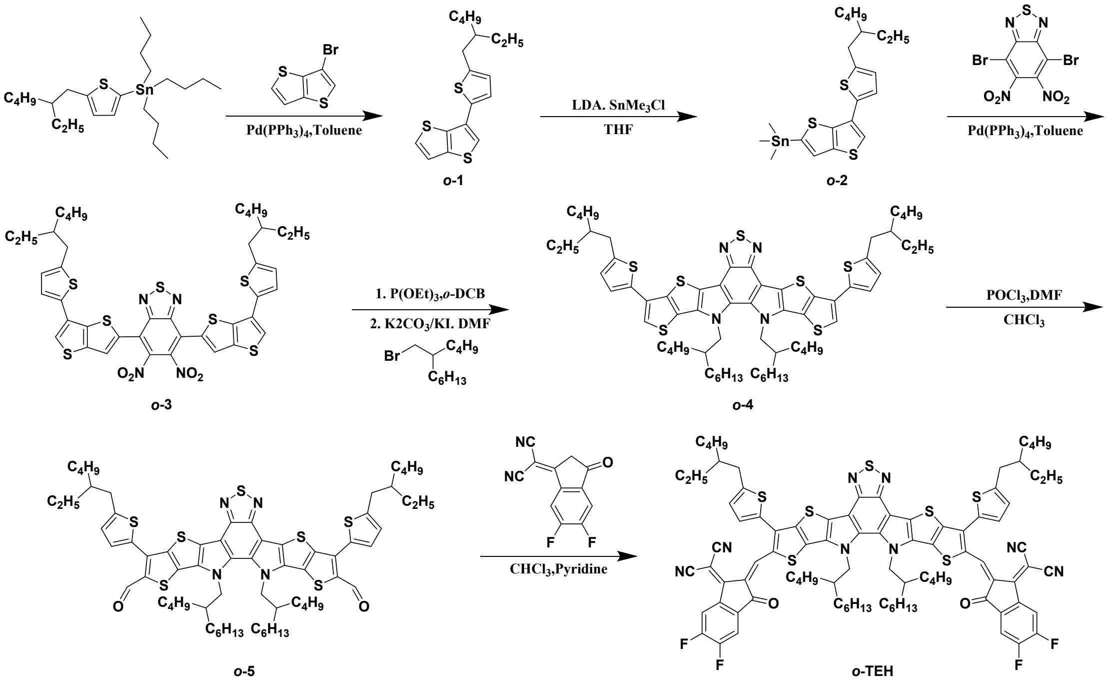

Scheme S2. Synthetic route of the *o*-TEH

Synthetic route of *o*-TEH is shown in **Scheme S2**. The detailed synthesis processes are described in the following.

Synthesis of compound *o*-1

A mixture of compound tributyl(5-(2-ethylhexyl)thiophen-2-yl)stannane (4.00 g, 8.24 mmol), 3-bromothieno[3,2-b]thiophene (1.85 g, 8.45 mmol), and $Pd(PPh_3)_4$ (0.35 g, 0.30 mmol) were dissolved in anhydrous toluene (40.0 mL) and stirred at 110 °C overnight under argon atmosphere. After being cooled to room temperature, the solvent was then removed under reduced pressure. The residue was washed with water and extracted with hexane. Without any further purification, the product was used into the following reaction.

Synthesis of compound *o*-2

To a solution of compound ***o*-1** in anhydrous tetrahydrofuran (40 mL), 2.0 **M** lithium diisopropylamide (3.0 mL, 6.0 mmol) was added dropwise at -78 °C under argon atmosphere. After stirring at the same temperature for 3.5 h, 1.0 **M** trimethyltin chloride (6.0 mL, 6.0 mmol) was added dropwise at -78 °C, and the mixture was gradually warmed to room temperature. After stirring overnight, the mixture was quenched with saturated KF aqueous solution and extracted with hexane. The organic layer was dried with Na_2SO_4. Removing the solvent under reduced pressure gave the crude compound ***o*-2**. Without any further purification, the product was used into the following reaction.

Synthesis of compound *o*-3

Compound ***o*-2**, 4,7-dibromo-5,6-dinitrobenzo[c][1,2,5]thiadiazole (0.96 g, 2.5 mmol), and $Pd(PPh_3)_4$ (0.20 g, 0.17 mmol) were dissolved in anhydrous toluene(25.0 mL) and stirred at 110 °C overnight under argon atmosphere. Then, the reaction mixture was cooled and poured into a saturated KF aqueous solution. The mixture was extracted with diethyl ether for three times. The combined organic phase was washed with water followed by brine. Then, the solution was dried over Na_2SO_4 and concentrated under reduced pressure. Compound ***o*-3** was purified by chromatography in on a silica gel column eluting with petroleum ether/dichloromethane (3/1, *v*/*v*), which yielding a red powder as product (1.69 g, 76% yield). ^{1}H NMR (300 MHz, $CDCl_3$) δ 7.73 (s, 2H), 7.54 (s, 2H), 7.23 (d, J = 3.6 Hz, 2H), 6.78 (d, J = 3.6 Hz, 2H), 2.79 (d, J = 6.7 Hz, 4H), 1.65 (dq, J = 9.6, 4.6, 2.4 Hz, 3H), 1.46 – 1.22 (m, 19H), 0.91 (td, J = 7.4, 4.4 Hz, 14H). ^{13}C NMR (75 MHz, $CDCl_3$) δ 152.25, 144.74, 142.01, 141.59, 139.59, 134.34, 131.11, 128.86, 126.06, 124.13, 123.90, 123.87, 123.70, 121.50, 119.54, 41.61, 34.33, 32.53, 29.02, 28.42, 26.92, 25.71, 23.16, 17.44, 14.29, 13.74, 11.00.

Synthesis of compound *o*-4

Compound ***o*-3** (1.69 g, 1.90 mmol) and triethyl phosphate (10 mL) were dissolved in anhydrous 1,2-dichlorobenzene (*o*-DCB, 10 mL) under argon and the mixture was stirred at 180 °C overnight. After cooling to room temperature, the solvent was removed by vacuum distillation. Subsequently, the red intermediate was then mixed with K_2CO_3 (2.63 g, 19.0 mmol), KI (0.32 g, 1.90 mmol), 5-(bromomethyl)decane (1.42 g, 5.70 mmol), and anhydrous DMF (25 mL) were mixed under argon and stirred at 100 °C overnight. The mixture was extracted with ethyl acetate ether for three times. The combined organic phase was washed with water followed by brine. Then, the solution was dried over Na_2SO_4 and concentrated under reduced pressure to yield an orange oil. Compound ***o*-4** was obtained by column chromatography on silica gel using petroleum ether/dichloromethane (6/1, *v*/*v*) as the eluent to give an orange solid (1.08 g, 49% yield). ^{1}H NMR (300 MHz, CDCl$_3$) δ 7.41 (s, 2H), 7.38 (d, J = 3.5 Hz, 2H), 6.83 (d, J = 3.5 Hz, 2H), 4.63 (d, J = 7.8 Hz, 4H), 4.03 (d, J = 5.9 Hz, 2H), 2.82 (d, J = 6.7 Hz, 4H), 2.19 – 2.00 (m, 2H), 1.65 (q, J = 6.0 Hz, 3H), 1.49 – 1.19 (m, 34H), 1.19 – 0.52 (m, 67H). ^{13}C NMR (75 MHz, CDCl$_3$) δ 147.62, 144.43, 139.37, 136.67, 134.47, 131.93, 130.25, 125.93, 124.33, 124.08, 118.02, 111.61, 70.80, 55.14, 41.55, 38.76, 37.45, 34.25, 32.44, 31.82, 31.54, 31.01, 30.68, 30.42, 30.31, 30.18, 29.61, 29.33, 29.31, 28.92, 28.88, 28.03, 27.86, 26.64, 25.60, 25.35, 25.16, 23.04, 22.98, 22.76, 22.72, 22.65, 22.46, 22.44, 14.16, 14.09, 14.05, 13.94, 13.92, 13.76, 13.72, 10.89.

Synthesis of compound ***o*-5**

Compound ***o*-4** (1.08 g, 0.93 mmol) was dissolved in 20 mL trichloromethane under argon, then the fresh Vilsmeier reagent (3.4 mL POCl$_3$ in 7.2 mL DMF) was added dropwise at 0 °C. After stirring for 20 min at 0 °C, the mixture was heated to 65 °C and reacted 24 hours. The reaction was quenched with saturated NaHCO$_3$ solution and allowed to stir at room temperature for 24 hours. The organic layer was separated, and the aqueous phase was extracted with diethyl ether for three times. The combined organic layer was washed with brine, dried over Na$_2$SO$_4$, filtered, and concentrated under reduced pressure. The crude product was purified with column chromatograph on silica gel using petroleum ether/dichloromethane (1/1, *v*/*v*) as the eluent to give an orange solid ***o*-5** (907.6 mg, 80% yield). ^{1}H NMR (300 MHz, CDCl$_3$) δ 10.26 (s, 2H), 7.44 (d, J = 3.6 Hz, 2H), 6.94 (d, J = 3.6 Hz, 2H), 4.66 (d, J = 8.1 Hz, 4H), 2.88 (d, J = 6.8 Hz, 4H), 2.06 (p, J = 6.4 Hz, 2H), 1.69 (q, J = 6.2 Hz, 2H), 1.51 – 1.20 (m, 18H), 1.20 – 0.41 (m, 60H). ^{13}C NMR (75 MHz, CDCl$_3$) δ 183.76, 149.03, 147.50, 142.45, 138.01, 136.82, 136.58, 133.01, 130.48, 129.74, 129.27, 126.51, 112.52, 55.39, 41.57, 39.00, 34.34, 32.47, 31.51, 30.41, 30.25, 30.06, 29.34, 29.31, 28.89, 28.00, 27.82, 25.67, 25.25, 25.05, 23.02, 22.77, 22.73, 22.47, 22.45, 14.16, 13.95, 13.93, 13.75, 13.72, 10.88.

Synthesis of compound *o*-TEH

Compound ***o*-5** (50.0 mg, 0.04 mmol), 2-(5, 6-difluoro-3-oxo-2, 3-dihydro-1H-inden-1-ylidene) malononitrile (110.7 mg, 0.48 mmol), pyridine (1.0 mL), and chloroform (10.0 mL) were dissolved in a round bottom flask under nitrogen. The mixture was stirred at room temperature overnight, then the mixture was poured into methanol and filtered. The residue was purified with column chromatography on silica gel using dichloromethane/petroleum ether (1/1, v/v) as the eluent to give a dark blue solid ***o*-TEH** (50.6 mg, 77% yield). ^{1}H NMR (300 MHz, CDCl$_3$) δ 9.13 (s, 2H), 8.52 (dd, J = 10.0, 6.4 Hz, 2H), 7.70 (t, J = 7.6 Hz, 2H), 7.38 (d, J = 3.6 Hz, 2H), 7.03 (d, J = 3.6 Hz, 2H), 4.76 (dd, J = 8.2, 4.1 Hz, 4H), 2.92 (d, J = 6.8 Hz, 4H), 2.14 (p, J = 6.6 Hz, 2H), 1.73 (p, J = 6.1 Hz, 2H), 1.42 (dt, J = 22.3, 7.2 Hz, 16H), 1.30 – 0.48 (m, 59H). ^{13}C NMR (75 MHz, CDCl$_3$) δ 185.72, 158.89, 151.43, 147.50, 144.40, 143.93, 138.67, 137.54, 136.68, 134.88, 134.38, 134.12, 132.79, 132.44, 131.74, 130.62, 127.54, 121.25, 114.70, 113.87, 113.53, 112.34, 69.36, 55.75, 41.72, 39.32, 34.52, 32.42, 31.59, 30.61, 30.49, 30.37, 29.45, 29.41, 28.94, 28.15, 27.96, 25.58, 25.46, 25.25, 23.04, 22.87, 22.82, 22.50, 22.47, 14.20, 14.01, 13.99, 13.81, 13.77, 10.89.

2. Characterization of materials

^{1}H NMR and ^{13}C NMR spectra were recorded using a Bruker AV-300 spectrometer in a *d*–chloroform solution at 300 K, unless specified otherwise. Chemical shifts are reported as δ values (ppm) with tetramethylsilane (TMS) as a benchmark. UV-Vis absorption spectra were recorded on the Hitachi U-3010 UV-vis spectrophotometer. For solution absorption, *m*-TEH, *o*-TEH and PBQ6 are dissolved in chloroform. For the film measurements, *m*-TEH, *o*-TEH and PBQ6 solutions in chloroform were spin-coated on quartz plates.

The cyclic voltammetry measurement was performed on the Zahner IM6e electrochemical workstation, using a glassy carbon electrode as the working electrode, platinum wire as the counter electrode and Ag/AgCl as the reference electrode, at a potential scanning rate of 50 $mV\cdot s^{-1}$ in 0.1 M tetrabutylammonium hexafluorophosphate (Bu_4NPF6) acetonitrile solution. The ferrocene/ferrocene (Fc/Fc^{+}) pair was used as an internal reference.

3. Simulation details

All calculations are performed by ORCA (*version 5.0.1*)[1]. The geometries were optimized under PBEh-3c with a built-in modified double-zeta basis set, def2-mSVP. The energy levels were calculated with B3PW91 function using def2-TZVP basis set, the TDDFT calculations involved with exited states were calculated under B3LYP/def2-TZVP level[2]. The wavefunction analysis were performed by Multiwfn (*version 3.6*)[3]. VMD (*version 1.9.3*) was used for visualization[4].

4. Fabrication and characterization of OSCs

The structure of all OSCs adopts the conventional device structure, namely ITO/PEDOT: PSS/active layer/PDINN/Ag structure. The pre-patterned ITO glass substrate (sheet resistance = 15 Ω sq^{-1}) was sonicated sequentially in detergent, deionized water, acetone, and isopropanol, and then subjected to 25 minutes in an ultraviolet ozone chamber (Jelight Company, USA) UV treatment. Filter the PEDOT:PSS aqueous solution (Baytron P 4083, from HCStarck) through a 0.45mm filter, and pre-coat it on the pre-cleaned ITO glass at 7000 rpm for 30 seconds, and then heat the ITO substrate in the air at 150°C annealing for 0.5 h. The PBQ6:SMA (D:A=1:1.2, 18 mg mL^{-1} in total) was dissolved in chloroform (CF) with 1-chloronaphthalene (CN) (0.4%, v/v) additive. The blended solution was spin-coated on the PEDOT:PSS layer at 2700 rpm for 30s. It is then annealed at 90°C for 5 minutes. Then PDINN methanol solution with a concentration of 1.0 mg mL^{-1} was deposited on the active layer at a speed of 5000 rpm for 30 seconds to provide a PDINN cathode modification layer. After cooling to room temperature, the sample was transferred to the evaporation chamber. Under the pressure of 1×10^{-5} Pa, about 100 nm of Ag electrode was evaporated and deposited. The device area is 6.0 mm^2.

The current density–voltage (*J-V*) characteristics of OSC are measured in a nitrogen glove box equipped with a Keithley 2450 Source Measure Unit in a glove box filled with nitrogen (oxygen and water contents are smaller than 0.1 ppm), using Oriel Sol3A Class AAA Solar Simulator (model, Newport 94023A) with 450W xenon lamp and air quality (AM) 1.5 filter as the light source. The light intensity is calibrated to 100 mW cm^{-2} by Newport Oriel 91150V reference cell. The external quantum efficiency

(EQE) value is measured by the solar cell spectral response measurement system QE-R3-011 (Taiwan Enli Technology Co., Ltd.). Standard single-crystal silicon photovoltaic cells are used to calibrate the light intensity of each wavelength.

In the Photo-CLIVE, and TPV measures, the OSCs were fabricated with the same method as mentioned above. The data were obtained by the all-in-one characterization platform, Paios (Fluxim AG, Switzerland). In the photo-CELIV measurement, the delay time is set to 0 s, the light intensity is 100%, the light-pulse length is 100 μs, finally the sweep ramp rate rises from 20 V/ms to 100 V/ms. In the TPV measurement, the light intensity is 0.10%, 0.23%, 0.53%, 1.23%, 2.83%, 6.52%, 15.0%, 34.6% and 80.0%, respectively, relative intensity is 20.0% and settling time is 30.0 ms, pulse length is 5.0 ms and the follow-up time is 30.0 μs.

5. Hole mobility and electron mobility measurements

ITO/PEDOT:PSS/active layer/MoO_3/Ag device structure is used to test hole mobility, and ITO/ZnO/active layer/PDINN/Ag is used to test electron mobility. The hole and electron mobilities are calculated according to the space charge limited current (SCLC) method with the equation: $J = 9\mu\varepsilon_r\varepsilon_0 V^2 / 8d^3$, where J is the current density, μ is the hole or electron mobility, V is the internal voltage in the device, ε_r is the relative dielectric constant of active layer material, ε_0 is the permittivity of empty space, and d is the thickness of the active layer.

6. GIWAXS measurements and related discussion

Grazing-incidence wide-angle X-ray scattering (GIWAXS) measurements

GIWAXS measurements were performed on a XEUSS SAXS/WAXS system (XENOCS, France) at the National Center for Nanoscience and Technology (NCNST, Beijing).

Discussion on OOP (100) and IP (010) diffraction peaks: The (100) diffraction peaks of the *m*-TEH and *o*-TEH films in the OOP direction were located at 0.454 Å^{-1} (*d*-spacing: 13.845 Å) and 0.468 Å^{-1} (*d*-spacing: 13.419 Å) respectively, and the crystal coherence lengths (CCLs) of *m*-TEH and *o*-TEH films were 99.522 Å^{-1} and 47.214 Å, respectively. In addition, from the IP direction, there were (010) diffraction peaks at 1.352 Å^{-1} (*d*-spacing: 4.647 Å) for *m*-TEH and 1.376 Å^{-1} (*d*-spacing: 4.566 Å) for *o*-TEH, and the CCLs of *m*-TEH and *o*-TEH films were 32.888 Å and 29.089 Å, respectively. From the calculated results, we can see that *m*-TEH exhibits longer CCLs than *o*-TEH in both the lamellar stacking in the OOP direction and the π-π stacking in the IP direction, which means that *m*-TEH exhibits more ordered intermolecular packing than *o*-THE, which will facilitate the charge transport in the OSCs.

7. AFM and TEM measurements

The morphologies of the blend films were investigated by atomic force microscopy (AFM, Agilent Technologies, 5500 AFM/SPM System, USA) in contacting mode with a 5 μm scanner. Transmission electron microscope (TEM) measurements were performed in a JEM-2100F.

8. Transient absorption spectroscopy

Femtosecond transient absorption spectrometer was composed of a regenerative-amplified Ti: sapphire laser system (Coherent) and Helios pump-probe system

(Ultrafast Systems). The regenerative-amplified Ti: sapphire laser system (Legend Elite-1K-HE, center wavelength of 800 nm, pulse duration of 25 fs, pulse energy of 4 mJ, repetition rate of 1 kHz) was seeded with a mode-locked Ti: sapphire laser system (Vitara) and pumped with a Nd: YLF laser (Evolution 30). The output 800 nm fundamental of the amplifier was split into two beam pulses. The main part of the fundamental beam went through the optical parametric amplifiers (TOPAS-C), whose output light was set as the pump light with wavelength of 840 nm and chopped by a mechanical chopper operating at frequency of 500 Hz. A small part of the fundamental beam was introduced into the TA spectrometer in order to generate the probe light. After passing through a motorized optical delay line, the fundamental beam was focused on a sapphire crystal or YAG crystal, which was used to generate the white-light continuum (WLC) probe pulses with wavelength of 430 to 820 nm or 800 to 1600 nm, respectively. The optical path difference between the pump light and the probe light, which is controlled by the motorized optical delay-line, was used to monitor the transient states at different pump-probe delay. A reference beam was split from the WLC in order to correct the pulse-to-pulse fluctuation of the WLC. The pump was spatially and temporally overlapped with the probe beam on the sample. Excitation energy of the pump pulse was set to 2 $\mu J/cm^2$ to avoid singlet-singlet annihilation. The film samples for TA measurements were prepared by spin coating the corresponding materials on thin quartz plates. The film samples were thermally annealed the same way as the actual device.

Supplementary Figures

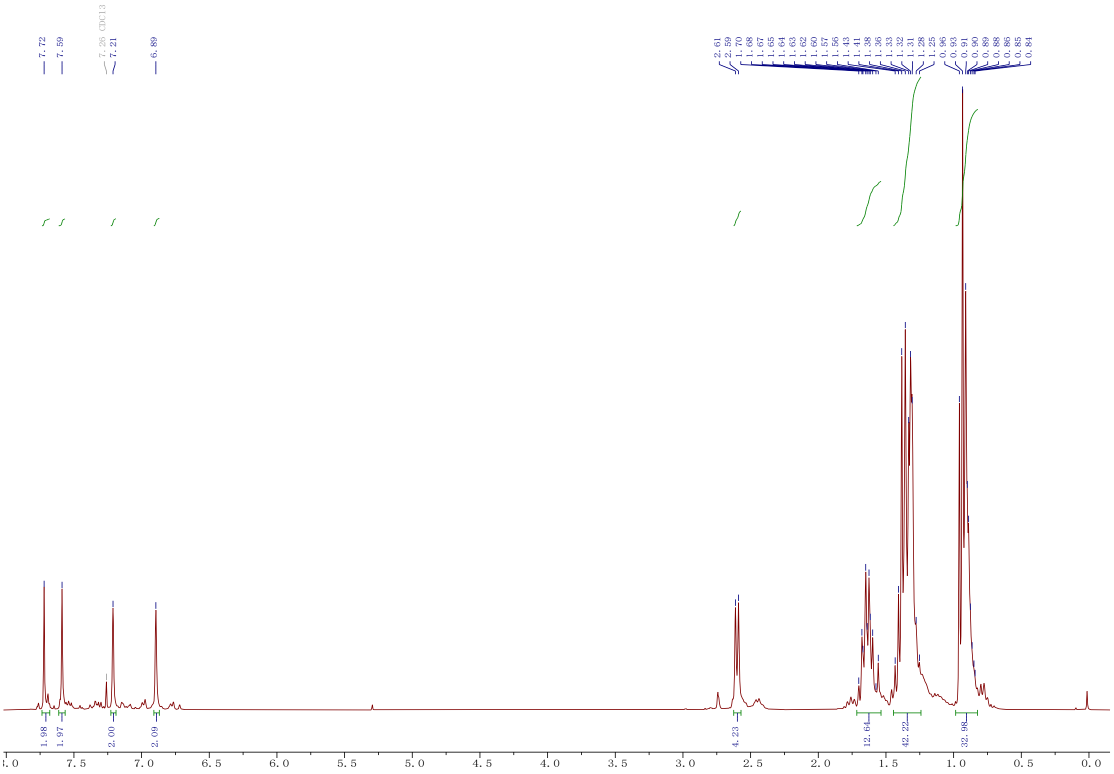

Fig. S1 ^{1}H NMR spectrum of ***m*-3** in $CDCl_3$.

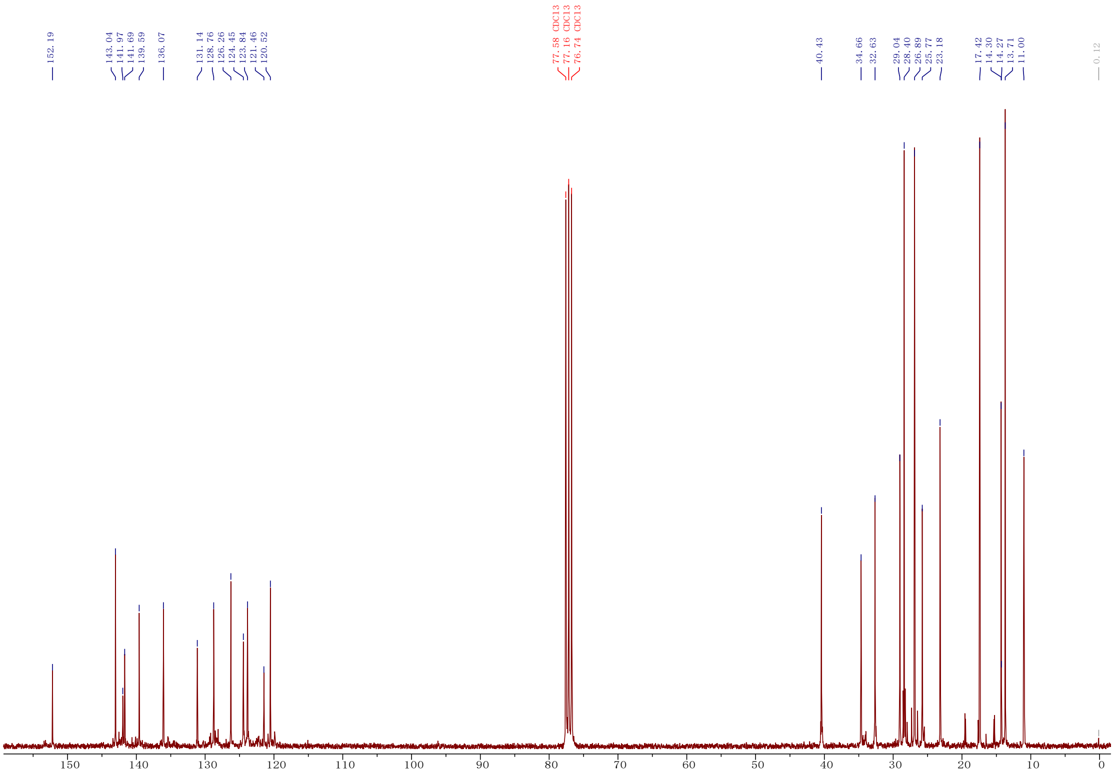

Fig. S2 ^{13}C NMR spectrum of ***m*-3** in $CDCl_3$.

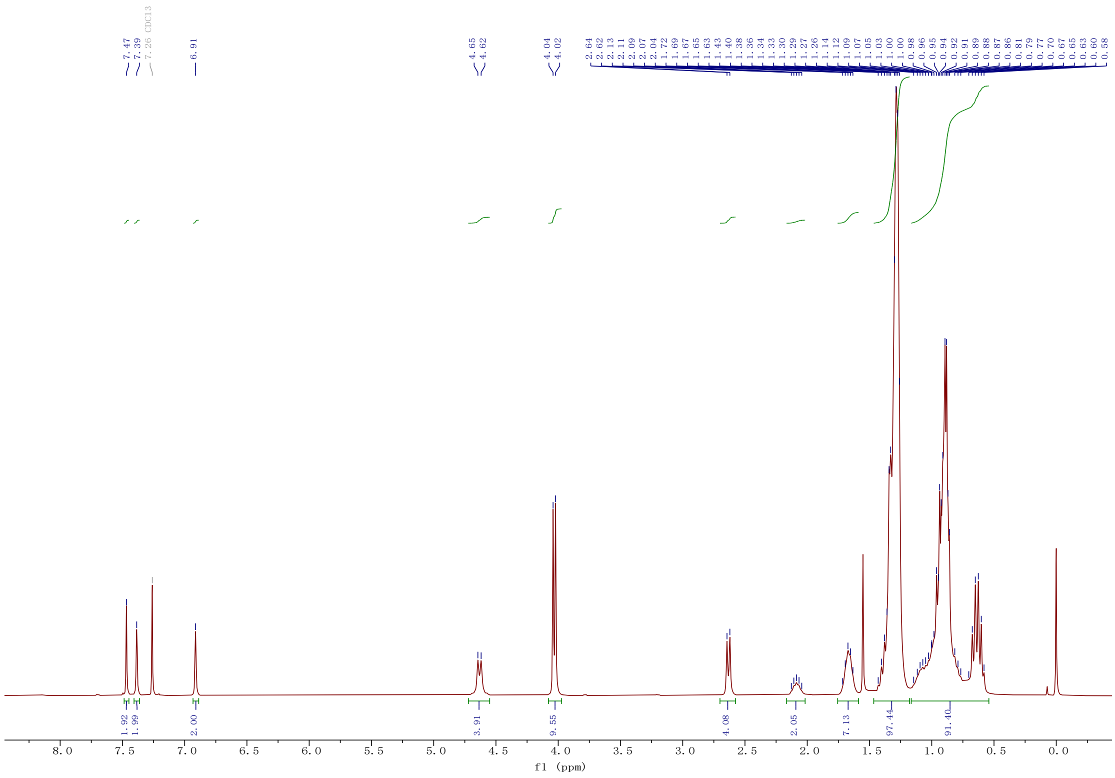

Fig. S3 ^{1}H NMR spectrum of ***m*-4** in CDCl$_3$.

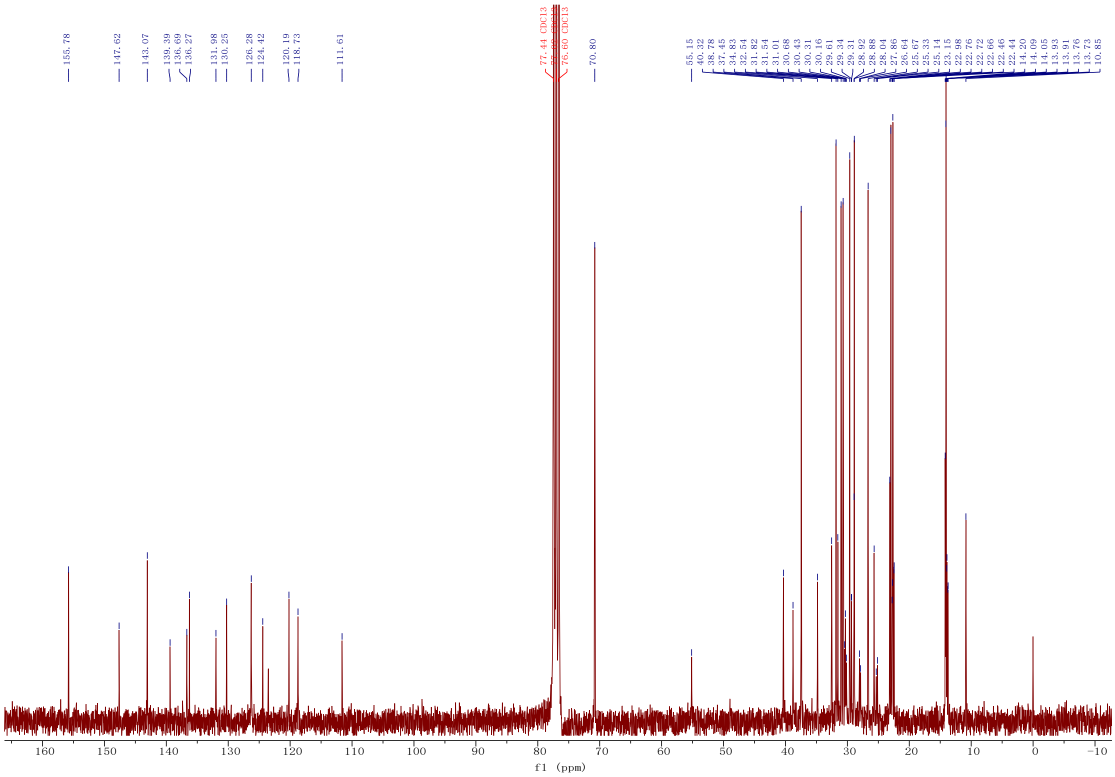

Fig. S4 ^{13}C NMR spectrum of ***m*-4** in CDCl$_3$.

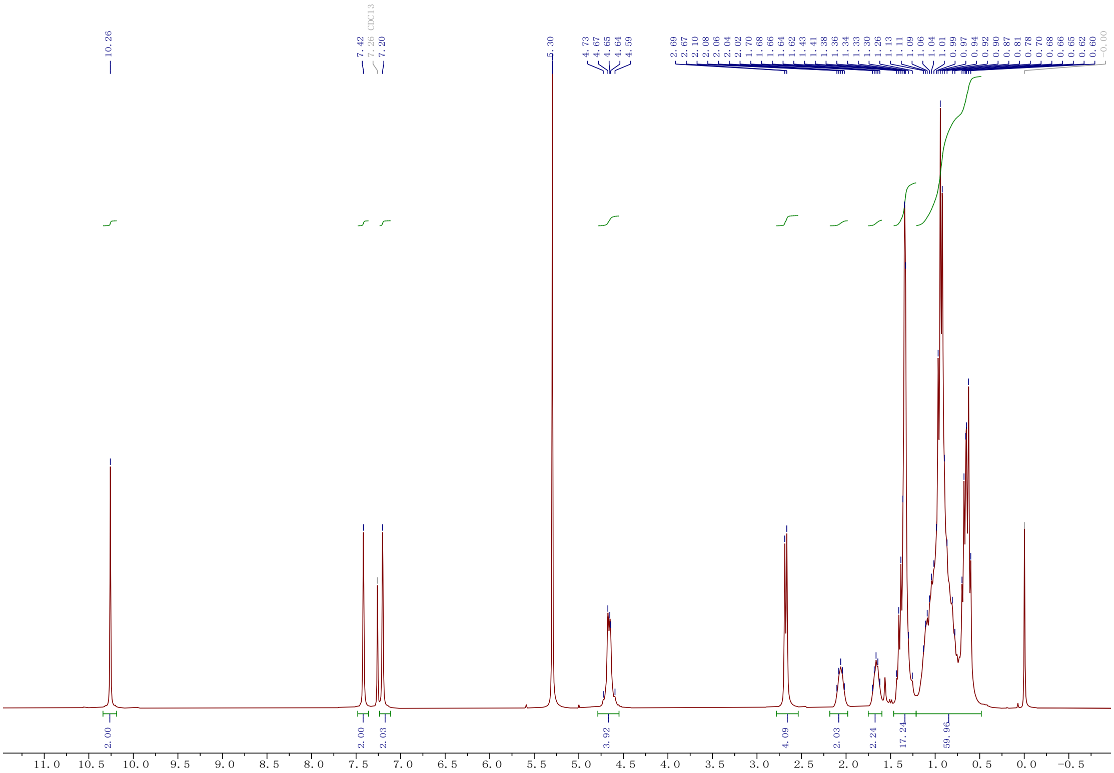

Fig. S5 ^{1}H NMR spectrum of ***m*-5** in $CDCl_3$.

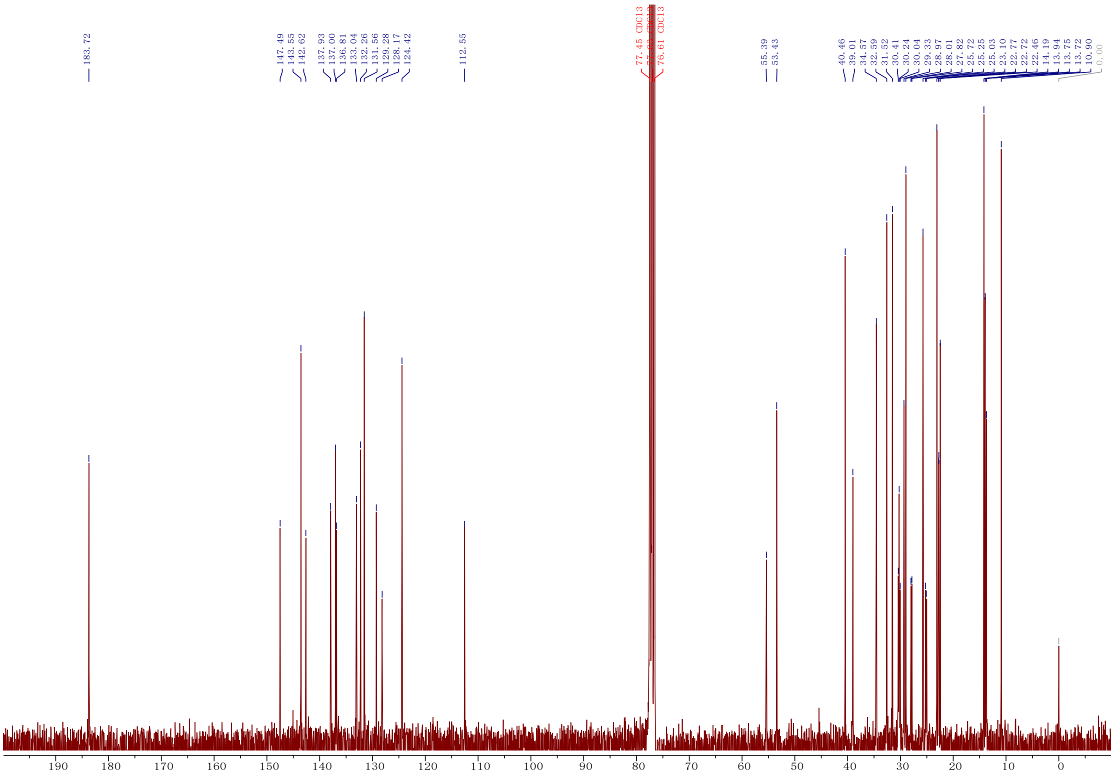

Fig. S6 ^{13}C NMR spectrum of ***m*-5** in $CDCl_3$.

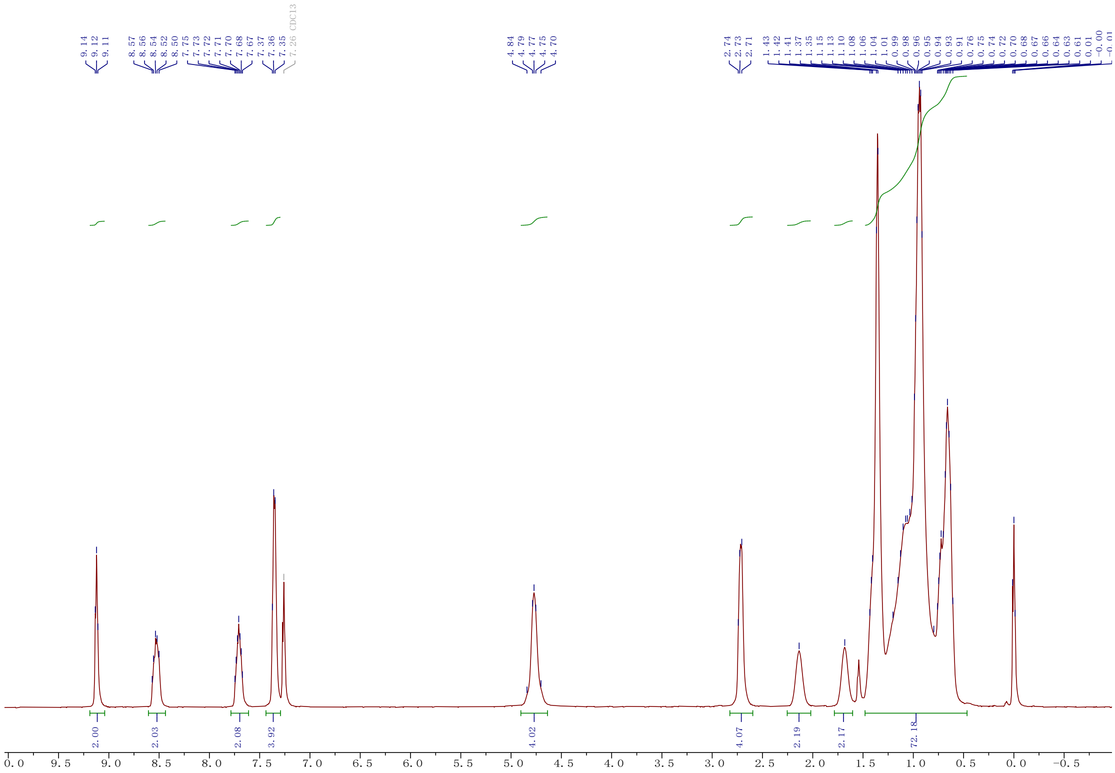

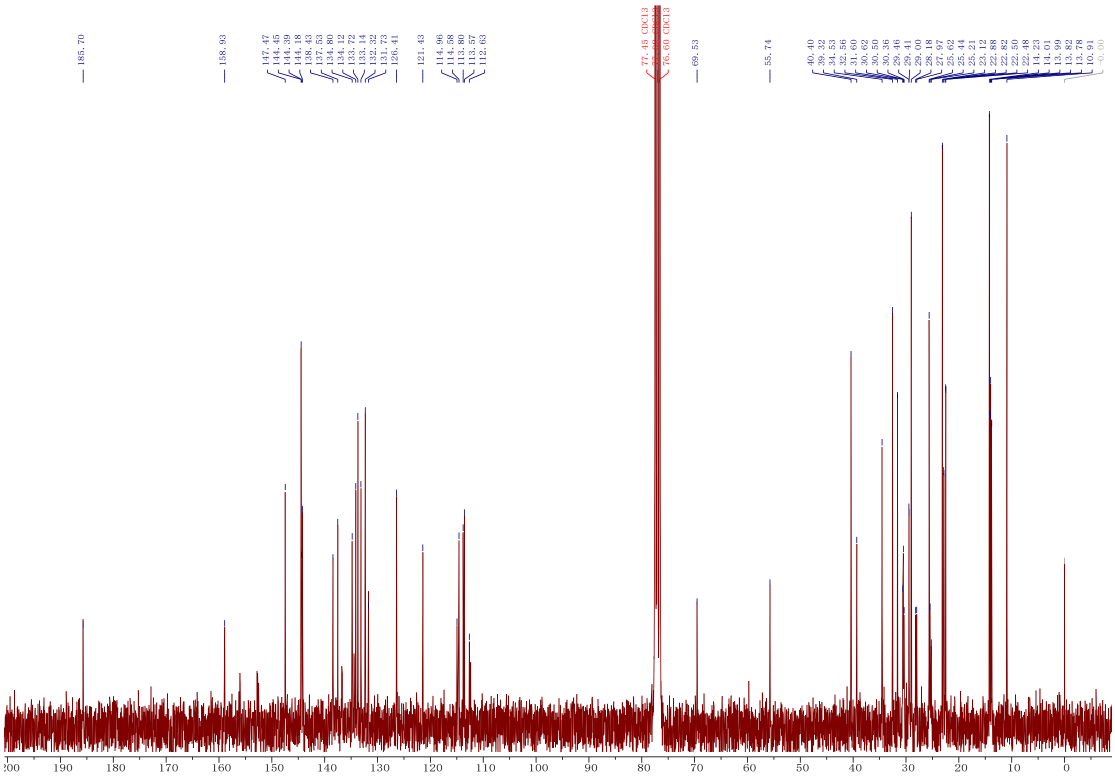

Fig. S7 ^{1}H NMR spectrum of ***m*-TEH** in $CDCl_3$.

Fig. S8 ^{13}C NMR spectrum of ***m*-TEH** in $CDCl_3$.

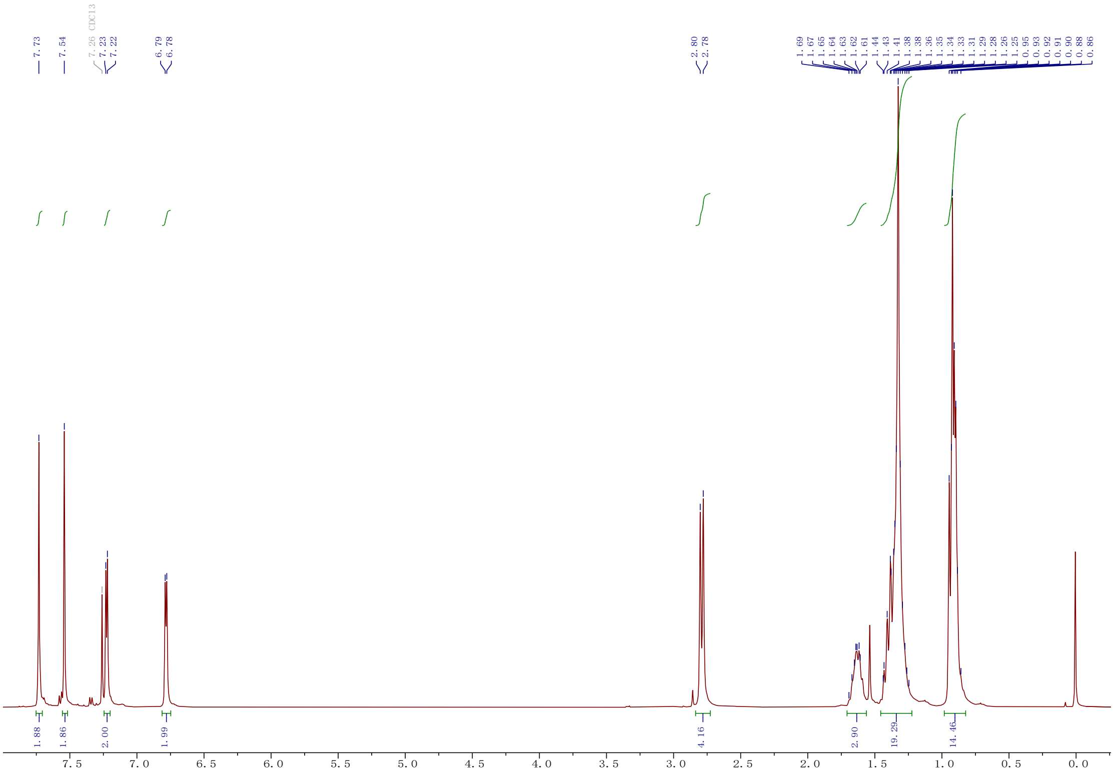

Fig. S9 ^{1}H NMR spectrum of ***o*-3** in $CDCl_3$.

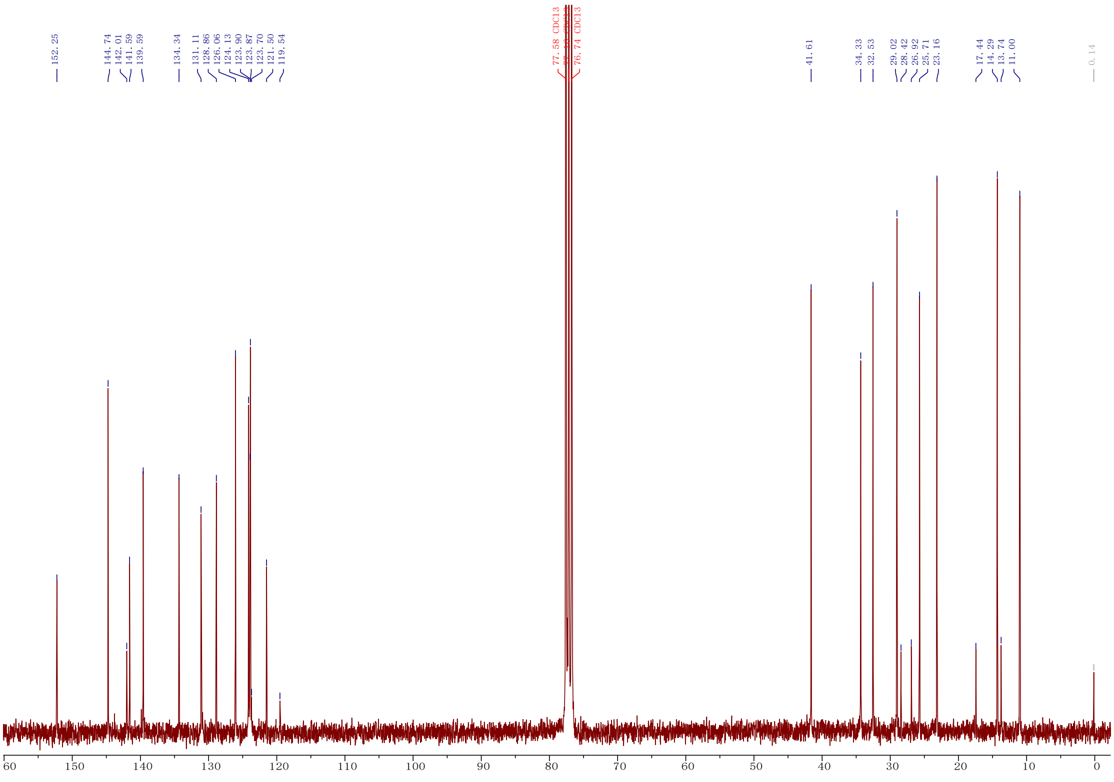

Fig. S10 ^{13}C NMR spectrum of ***o*-3** in $CDCl_3$.

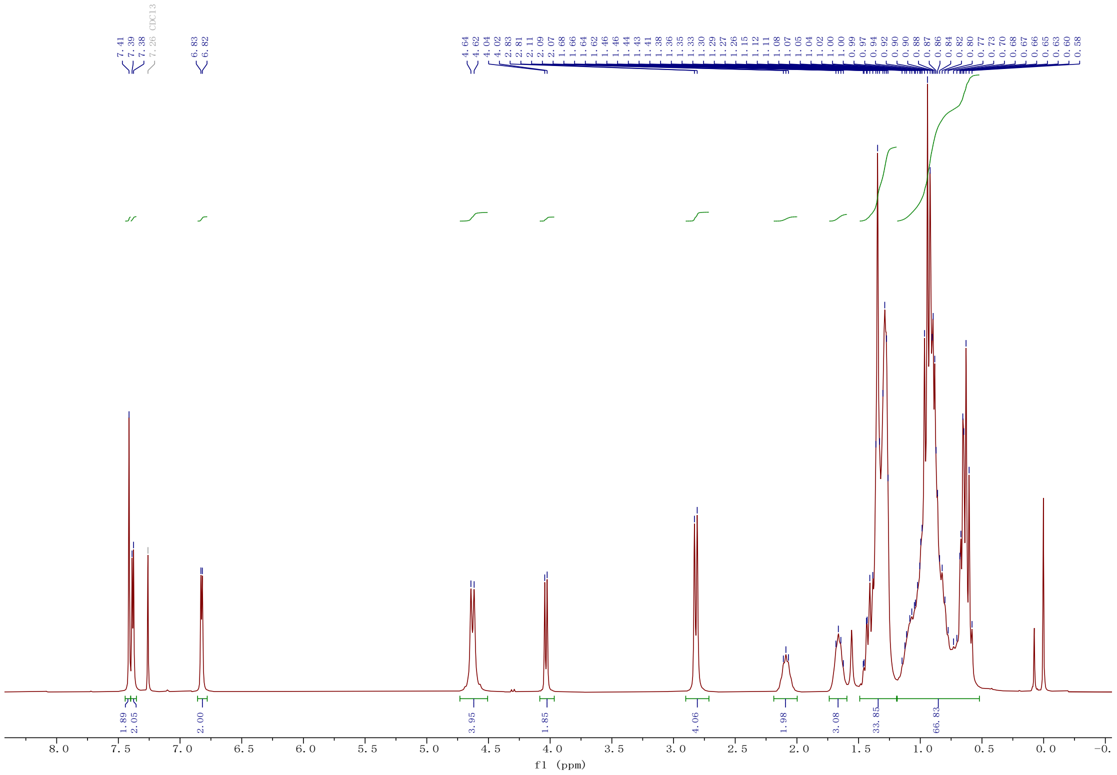

Fig. S11 ^{1}H NMR spectrum of ***o*-4** in CDCl$_3$.

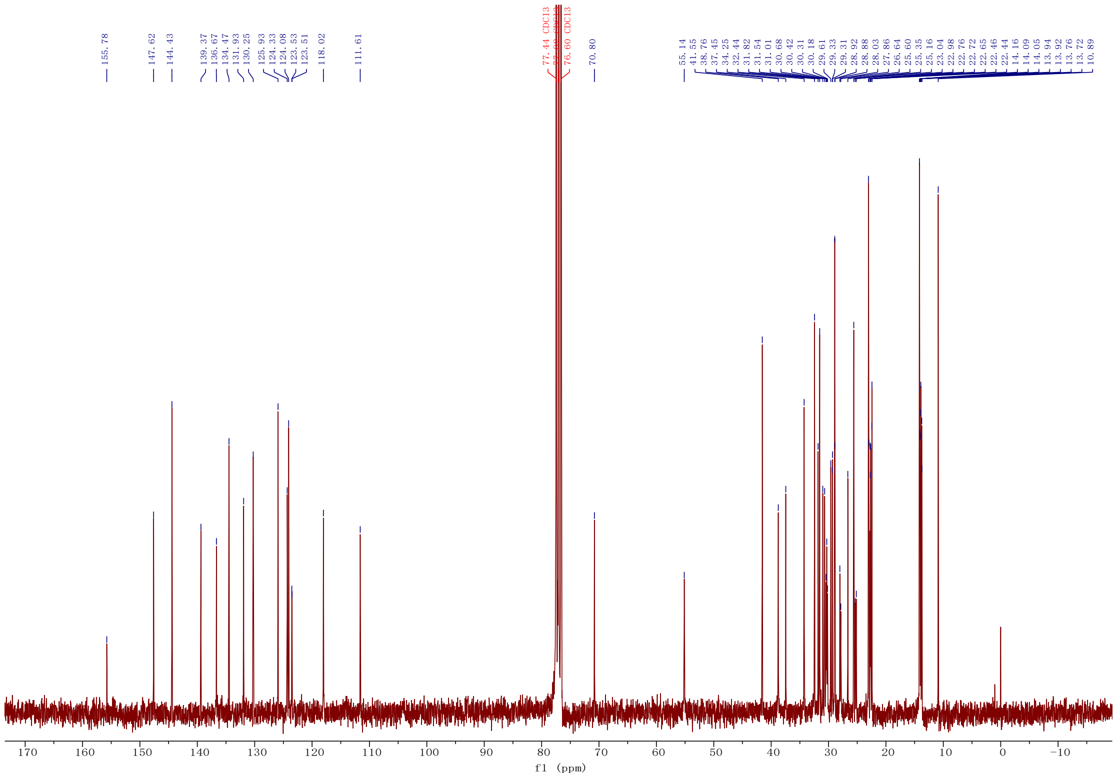

Fig. S12 ^{13}C NMR spectrum of ***o*-4** in CDCl$_3$.

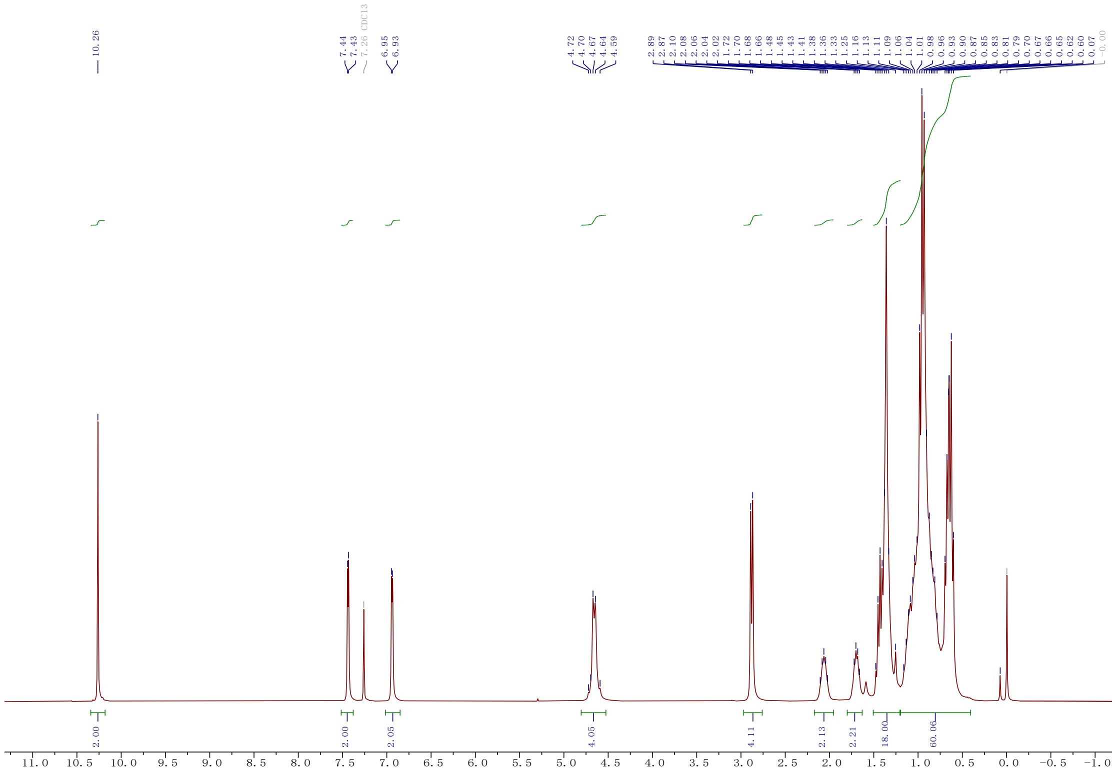

Fig. S13 ^{1}H NMR spectrum of ***o*-5** in $CDCl_3$.

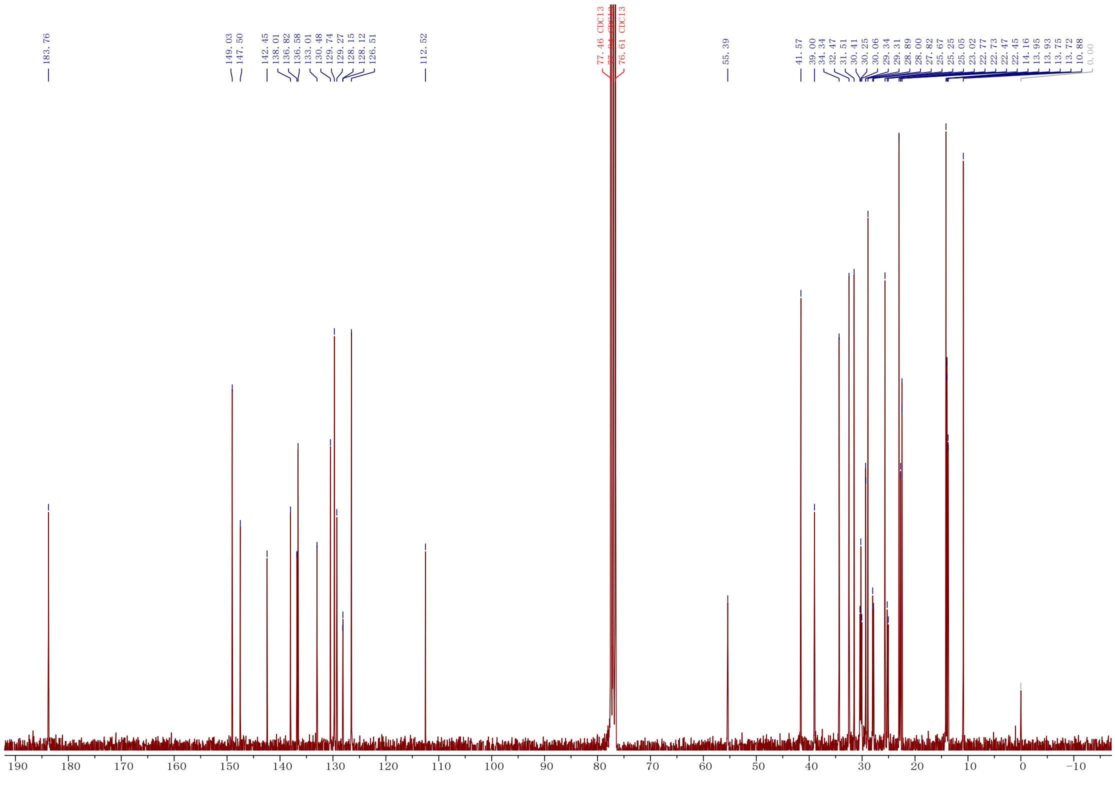

Fig. S14 ^{13}C NMR spectrum of ***o*-5** in $CDCl_3$.

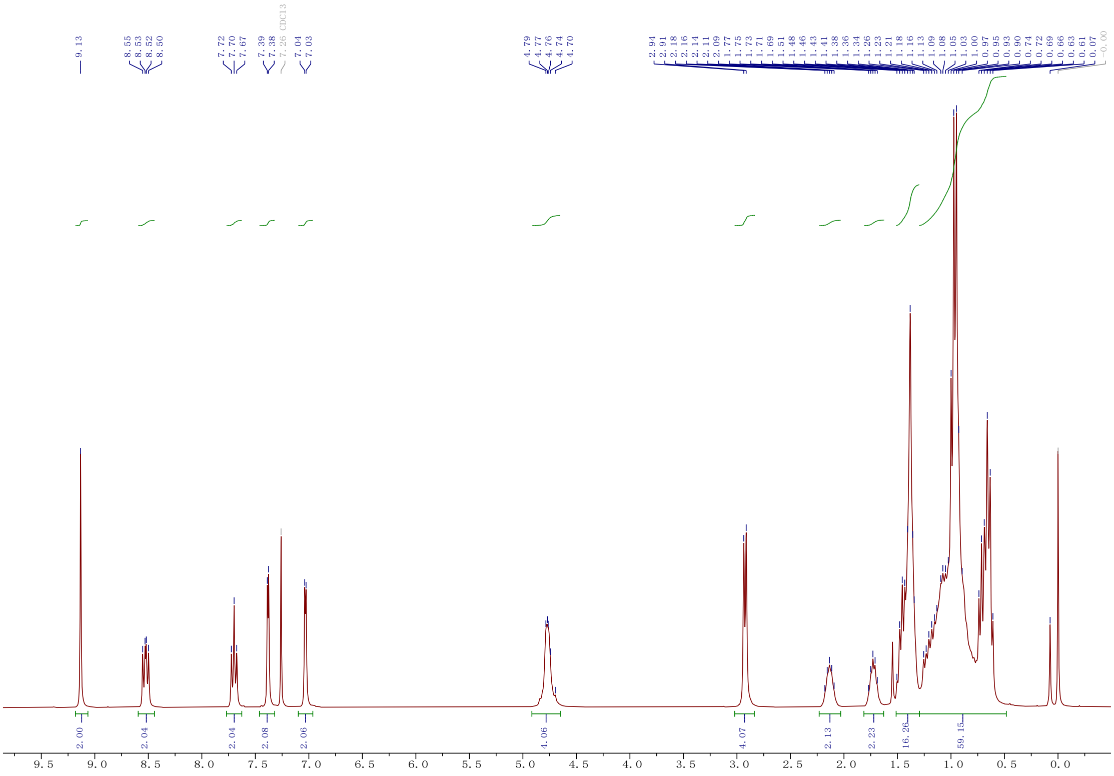

Fig. S15 ^{1}H NMR spectrum of ***o*-TEH** in $CDCl_3$.

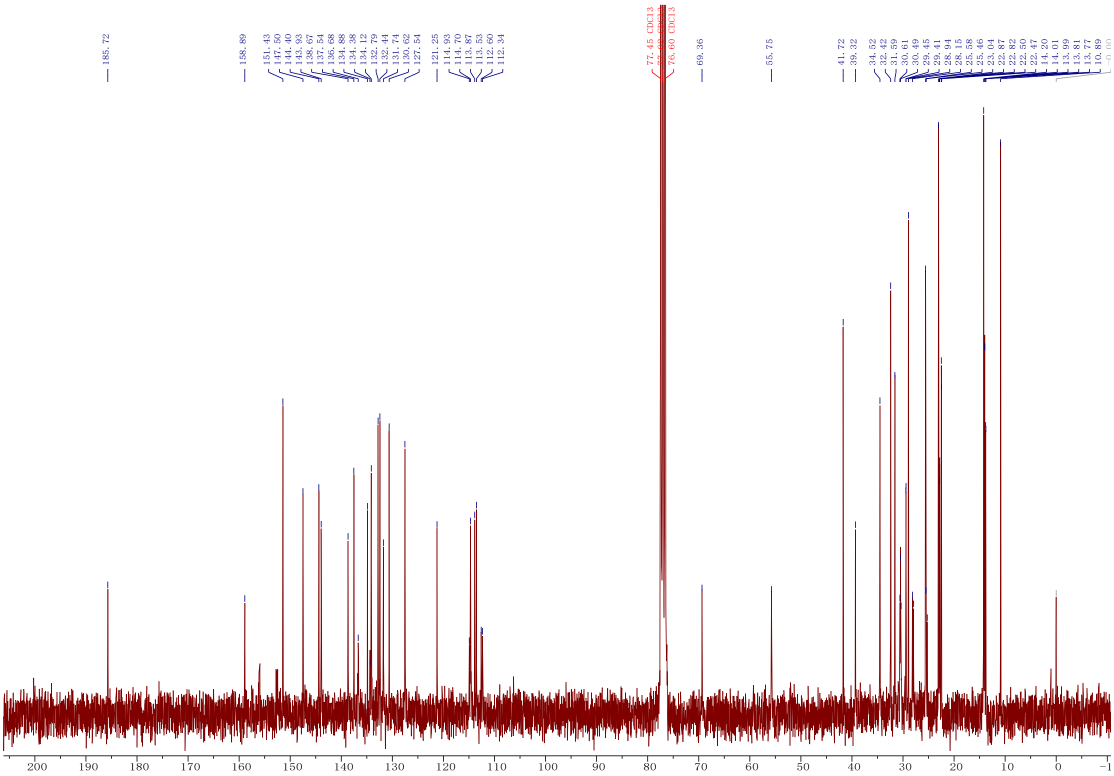

Fig. S16 ^{13}C NMR spectrum of ***o*-TEH** in $CDCl_3$.

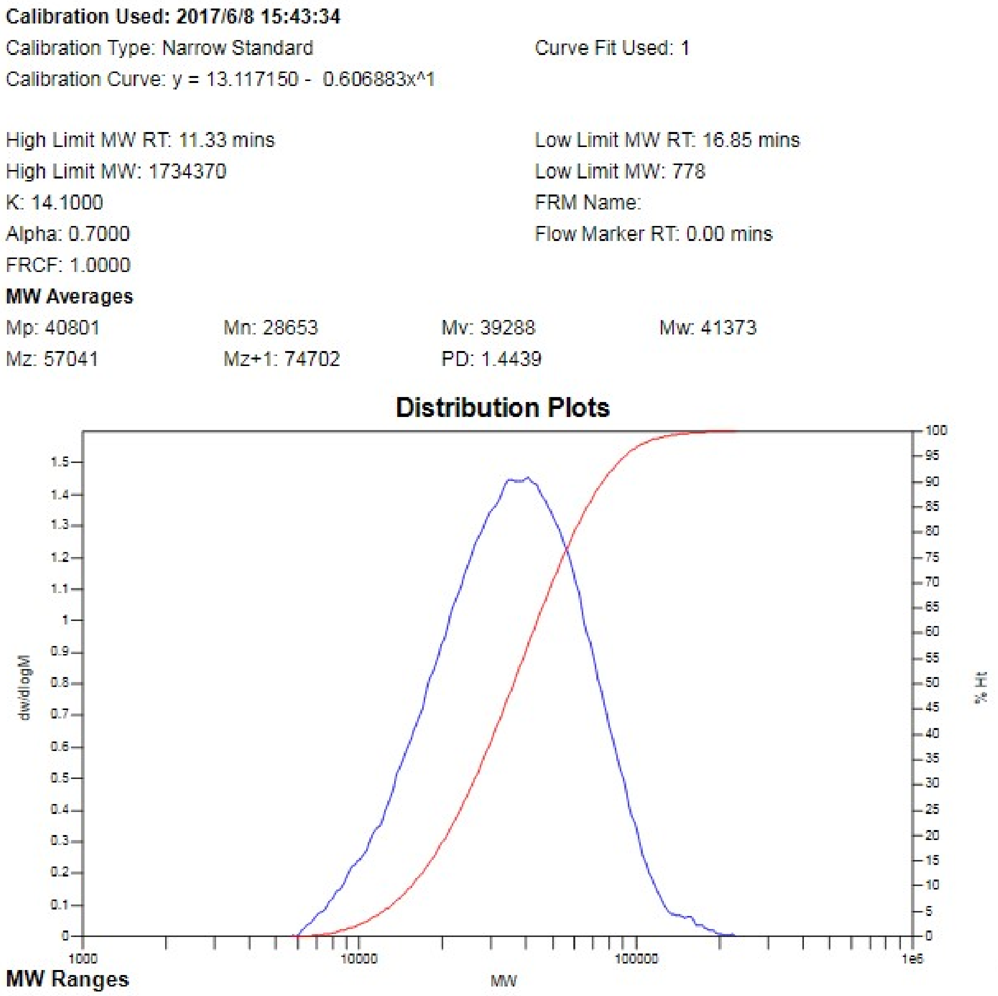

```
Calibration Used: 2017/6/8 15:43:34
Calibration Type: Narrow Standard                Curve Fit Used: 1
Calibration Curve: y = 13.117150 -  0.606883x^1

High Limit MW RT: 11.33 mins                     Low Limit MW RT: 16.85 mins
High Limit MW: 1734370                           Low Limit MW: 778
K: 14.1000                                       FRM Name:
Alpha: 0.7000                                    Flow Marker RT: 0.00 mins
FRCF: 1.0000
MW Averages
Mp: 40801          Mn: 28653          Mv: 39288          Mw: 41373
Mz: 57041          Mz+1: 74702        PD: 1.4439
```

```
MW Ranges
```

Fig. S17 The GPC chart related to the molecular weight of PBQ6.

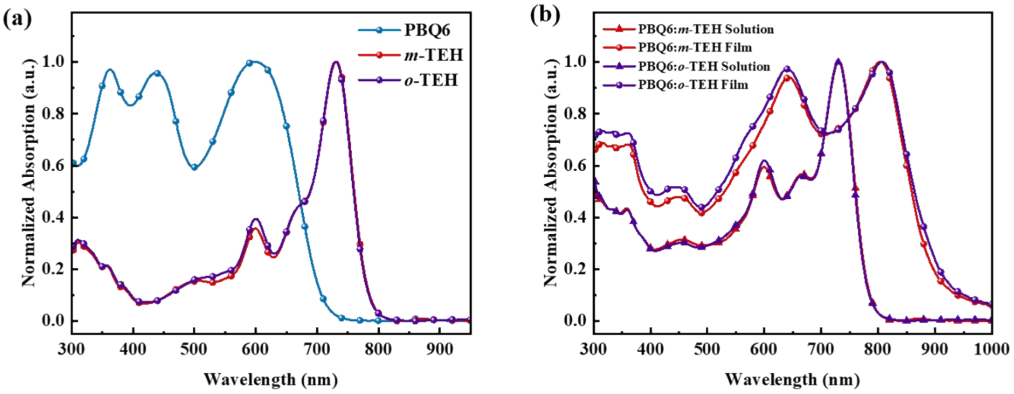

Fig. S18 (a) UV-vis absorption spectra of solutions (chloroform) of PBQ6, *m*-TEH and *o*-TEH. (b) UV-vis absorption spectra of solutions (chloroform) and films of PBQ6：*m*-TEH and PBQ6:*o*-TEH.

Fig. S19 Cyclic voltammograms of PBQ6, *m*-TEH and *o*-TEH.

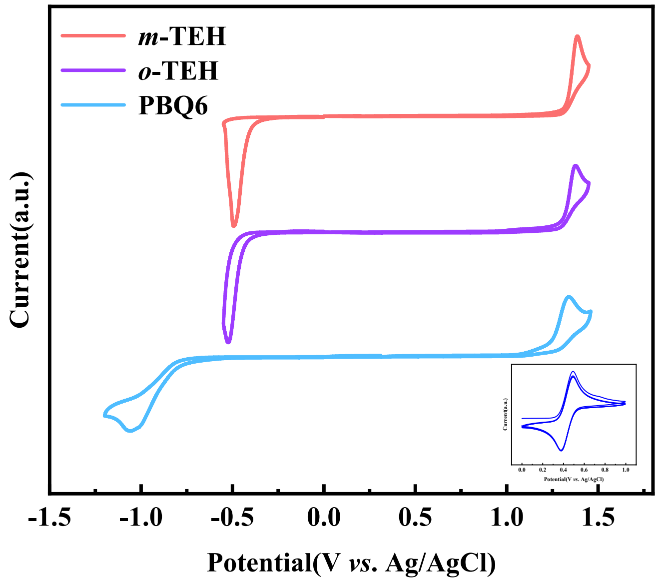

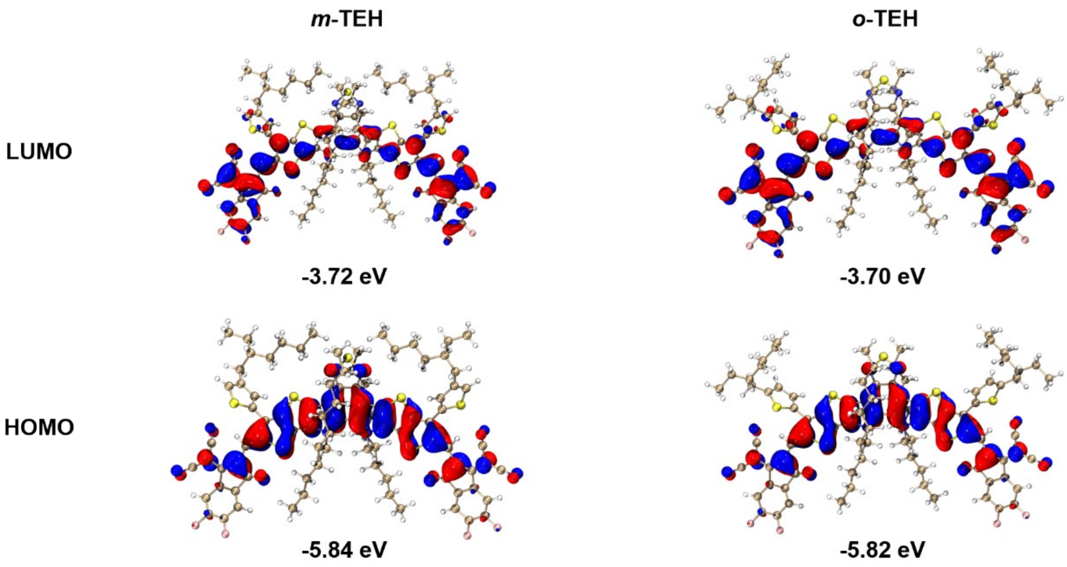

Fig. S20 Simulated frontier molecular orbital distribution of the two SMAs.

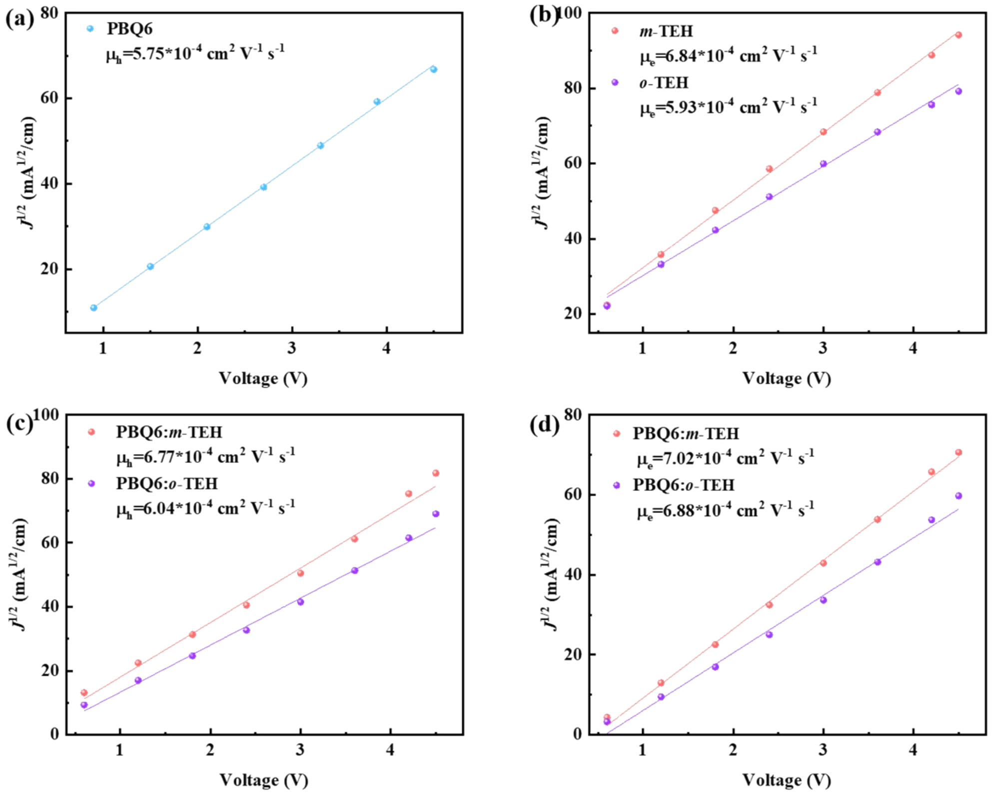

Fig. S21 $J^{1/2}$~V characteristics of the charge carrier mobility measurements of the neat films of PBQ6 (a), SMAs (b) and the blend films (c, d) in the dark.

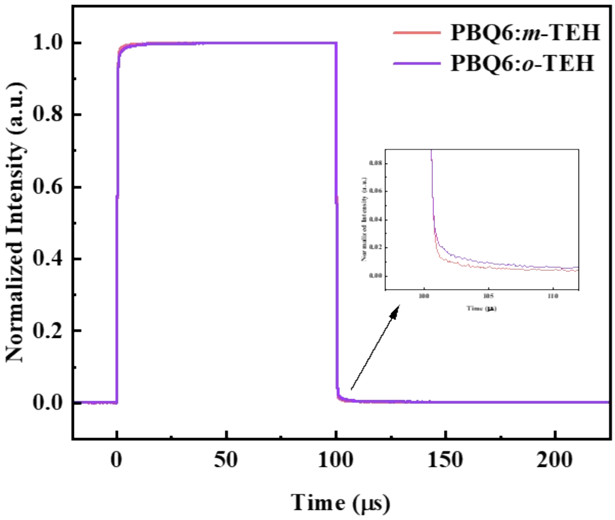

Fig. S22 Normalized transient photocurrents in response to a 100 μs white light (LED) pulse for devices.

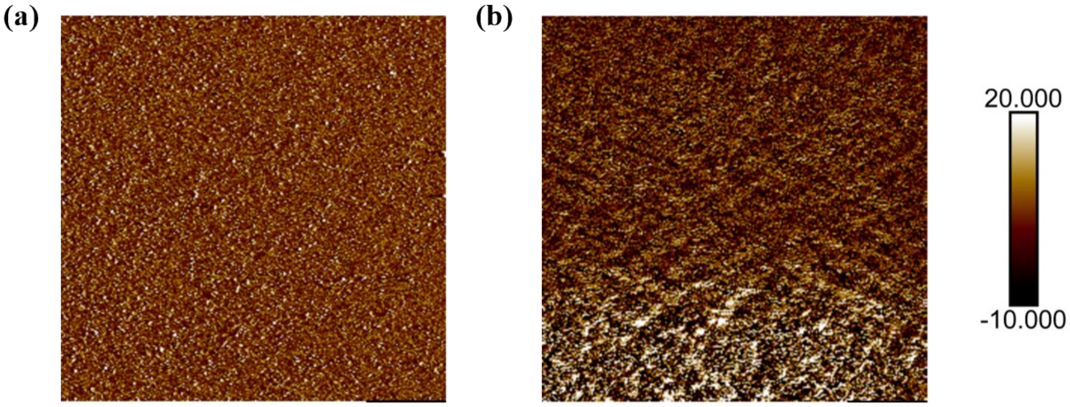

Fig. S23 AFM phase images (5 μm scale) of (a) PBQ6:*m*-TEH blend film and (b) PBQ6:*o*-TEH blend film.

Supplementary Tables

Table S1. Photovoltaic performance of the OSCs based on PBQ6:m-TEH with different device fabrication conditions, under the illumination of AM 1.5 G, 100 mWcm-2 (the active layer thickness is 115 nm).

Concentration (CF) (mg/mL)	**D/A Ratio**	**Additive (CN)** (%)	**Annealing** (°C)	V_{oc} (V)	J_{sc} (mA cm^{-2})	**FF** (%)	**PCE** (%)
18	1:1.2	0.4	80	0.883	26.37	78.59	18.30
			90	0.880	26.61	79.03	18.51
			100	0.876	26.28	78.82	18.15
		0.7	80	0.882	25.39	77.68	17.40
			90	0.877	25.59	77.95	17.49
			100	0.872	25.32	77.82	17.18
	1:1.4	0.4	80	0.881	26.17	78.02	17.99
			90	0.875	26.21	78.39	17.98
			100	0.870	26.08	78.25	17.75
		0.7	80	0.883	25.29	77.62	17.33
			90	0.879	25.69	77.85	17.60
			100	0.876	25.42	77.77	17.32

Table S2. Detailed data of the hole mobility (μ_h) and electron mobility (μ_e).

Active layer	μ_h^a (10^{-4} cm^2 V^{-1} s^{-1})	μ_e^a (10^{-4} cm^2 V^{-1} s^{-1})	μ_h/μ_e
PBQ6:*m*-TEH	6.77	7.02	0.96
PBQ6:*o*-TEH	6.04	6.88	0.88

[a]. average values obtained from more than ten different devices.

Table S3. GIWAXS measurement parameters of the related films.

Film	**In plane** **Location** ($Å^{-1}$)	**In plane** ***d*-spacing** (Å)	**In plane** **CCL** (Å)	**Out of plane** **Location** ($Å^{-1}$)	**Out of plane** ***d*-spacing** (Å)	**Out of plane** **CCL** (Å)
PBQ6	0.271	23.159	69.664	1.661	3.784	21.307
m-TEH	0.281/0.392	22.390/16.018	82.717/53.901	1.667	3.768	17.459
o-TEH	0.287/0.396	21.875/15.859	71.305/58.137	1.660	3.784	16.068
PBQ6:*m*-TEH	0.280	22.478	83.289	1.667	3.769	18.832
PBQ6:*o*-TEH	0.281	22.370	77.159	1.662	3.781	17.666

Notes and references

1. F. Neese, *WIREs Comput. Mol. Sci.*, 2012, **2**, 73–78.
2. S. Qin, L. Meng and Y. Li, *ACS Omega*, 2021, **6**, 14467–14475.
3. T. Lu and F. Chen, *J. Comput. Chem.*, 2012, **33**, 580–592.
4. W. Humphrey, A. Dalke and K. Schulten, *J. Mol. Graph.*, 1996, **14**, 33–38.